AIAA SciTech
13-17 January 2014, National Harbor, Maryland
AIAA Guidance, Navigation, and Control Conference

Simple Adaptive Control for Spacecraft Proximity Operations

Steve Ulrich,* Dustin Luke Hayhurst,† Alvar Saenz-Otero,‡ and David W. Miller§
Massachusetts Institute of Technology, Cambridge, Massachusetts, 02139

Itzhak Barkana¶
Barkana Consulting, 47209 Ramat-Hasharon, Israel

This paper addresses the problem of adaptive output feedback control for spacecraft proximity operations under parametric uncertainties and unknown disturbances. Control laws using the simple adaptive control theory, which is based on the so-called model reference adaptive control approach, are derived. In the first control scheme, a position feedback adaptive control law employing a parallel feedforward configuration to satisfy sufficient conditions guaranteeing closed-loop stability is developed. Then, it is shown how the performance of this adaptive controller can be significantly improved by using a position-plus-velocity feedback adaptive control strategy. Simulations compare the performance of the adaptive controllers with a fixed gain proportional-derivative controller. Obtained results demonstrate that both simple adaptive control methodologies yield improved performance, regardless of an uncertainty in the spacecraft mass and an unknown external perturbation, when compared to the linear-time invariant benchmark controller. In addition, the position-plus-velocity adaptive feedback methodology is shown to greatly reduce the required control input force, making its implementation onboard nanosatellites feasible. Finally, experiments conducted at the Massachusetts Institute of Technology's Synchronized Position Hold Engage Reorient Experimental Satellites research facility are reported and discussed.

I. Introduction

Spacecraft proximity operations represent an essential part of current and future space missions, including International Space Station (ISS) supply and repair, automated inspection, docking maneuvers, and on-orbit servicing.[1,2] Despite the success of a small number of experimental autonomous proximity operations in the previous decades, such as the Japanese Engineering Test Satellite VII (ETS-VII) in 1997, and the Orbital Express conducted by Defense Advanced Research Projects Agency (DARPA) in 2007,[3] such autonomous operations cannot be achieved routinely at present. For example, on July 24, 2012, the Progress-M unmanned cargo spacecraft experimenting with a new type of autopilot failed to autonomously rendezvous and dock with the ISS.[4] Such events highlight the fact that there is a need for more fundamental research and experimental work in the area of proximity operations, especially when operations with uncooperative or de-commissioned satellites are required.

For this reason, DARPA recently initiated the Phoenix program to develop and demonstrate a new class of very small modular *satlets*, similar to nanosatellites, to harvest valuable components from depleted satellites in geosynchronous orbits to assemble a new space system. As part of the first demonstration mission under this program, these small free-flyer spacecraft will be required to handle various components of different

*Postdoctoral Associate, Department of Aeronautics and Astronautics, 77 Massachusetts Avenue; now Assistant Professor, Department of Mechanical and Aerospace Engineering, Carleton University, Ottawa, Canada. Member AIAA.
†Graduate Student, Department of Aeronautics and Astronautics, 77 Massachusetts Avenue.
‡Research Scientist, Department of Aeronautics and Astronautics, 77 Massachusetts Avenue. Senior Member AIAA.
§Jerome C. Hunsaker Professor and Director of the Space Systems Laboratory, Department of Aeronautics and Astronautics, 77 Massachusetts Avenue. Associate Fellow AIAA.
¶President, 11 Hashomer Street. Associate Fellow AIAA.

masses, such as space apertures and antennas. In this context, the relative position control systems need to be robust to uncertainties in the free-flyer spacecraft mass, to ensure consistent and safe relative motion control with no trajectory overshoots.

Typically, in proximity operations, the spacecraft would be in sufficiently close proximity to enable the use of the Clohessy-Wiltshire (CW) equations,[5] or a simple double integrator model. These dynamics representations are particularly attractive for control purposes since they consist in a linear model of the spacecraft relative dynamics. For this reason, the literature proposes a large amount of linear control algorithms for rendezvous and docking applications. In particular, recent work at the Massachusetts Institute of Technology (MIT) reported successful experimental demonstrations of simple linear control algorithms for the spacecraft proximity operations problem.[6,7] However, most existing control techniques for rendezvous and proximity operations are model-based techniques and have reasonably good tracking performance only when substantial knowledge of the plant mathematical model and its parameters (e.g. spacecraft mass and inertia) is available. Consequently, if the spacecraft parameters are poorly known, or if there are unmodeled perturbations acting on the spacecraft, model-based control approaches could perform inadequately. For example, parameter uncertainties may arise from uncertain spacecraft mass-inertia properties which can change due to fuel consumption, solar array deployment, payload variation, or, in the context of DARPA's Phoenix program, when the spacecraft harvests a component of an unknown mass from the target satellite.

Recently, Yang et al.[8] managed parametric uncertainties by developing a robust control law. Their approach was based on the formulation - in the form of linear matrix inequalities (LMIs) - of existing conditions for admissible controllers, and on the casting of the controller design into a convex optimization problem subject to LMI constraints. Good control performance in spite of parametric uncertainties was demonstrated in a simple numerical simulation scenario. To cope with uncertainties in the plant parameters, indirect adaptive control techniques may also be employed as they identify in real time unknown plant parameters upon which the control gains are obtained using some automatic design procedure. However, this class of adaptive control methodologies nevertheless requires an accurate knowledge of the plant dynamics model.[9] For example, Singla et al.[10] proposed an indirect adaptive control strategy for docking with a cooperative target, in which an adaptation law based on an exact knowledge of the dynamics model identifies the unknown spacecraft mass that is used explicitly in their control law. An adverse consequence of such identification procedures is the increased computational burden associated with real-time estimation of unknown parameters. This drawback could rule out the use of such indirect adaptive controllers for space applications where available computational resources are limited.

Alternatively, direct adaptive control techniques, with the controller gains updated directly without requiring estimation of unknown plant parameters or mathematical models of the system to be controlled, can be used to address this problem. In view of the above discussion, the contribution of this work is to address the problem of spacecraft proximity operations under large mass uncertainties and unmodeled external disturbances through the use of direct adaptive control laws. More specifically, stable direct adaptive control strategies derived upon the simple adaptive control (SAC) theory[11] are proposed and validated through numerical simulations and experiments. The resulting adaptive control laws are robust, simple and easy to implement, making them suitable for a practical implementation within an onboard embedded computer.

This paper is organized as follows: Section II reviews the strict passivity and almost strict passivity conditions in linear time-invariant (LTI) systems. As it will be shown later in this paper, these conditions of the plant to be controlled are required for the derivation of the analytical proof of stability. Section III presents the simple adaptive control theory upon which both adaptive control strategies for the problem of spacecraft proximity operations are developed. In Section IV, a first adaptive control methodology using a position feedback is derived and evaluated in numerical simulations. Further improvements using a position-plus-velocity feedback adaptive control are discussed and assessed in simulations in Section V. Results obtained from experiments conducted at the MIT Space Systems Laboratory's Synchronized Position Hold Engage Reorient Experimental Satellites (SPHERES) research facility are reported in Section VI. Finally, Section VII provides a conclusion.

II. Strictly Passive and Almost Strictly Passive Systems

Consider an $m \times m$ square LTI plant described by the following standard state space formulation

$$\dot{x}_p = A_p x_p + B_p u_p, \qquad y_p = C_p x_p \tag{1}$$

where $x_p \in \mathbb{R}^n$ and $u_p, y_p \in \mathbb{R}^m$ are the plant states, control inputs and outputs, respectively, and A_p, B_p and C_p are appropriately dimensioned real matrices.

Definition 1: The LTI system described by Eq. (1) with the $m \times m$ transfer function given by $G_p(s) = C_p (sI - A_p)^{-1} B_p$ is strictly passive (SP) and its transfer function strictly positive real (SPR) if there exist two positive definite symmetric (PDS) matrices, denoted by P and Q, such that the following relationships are simultaneously satisfied[12]

$$PA_p + A_p^T P = -Q \tag{2}$$

$$PB_p = C_p^T \tag{3}$$

It is well known that the first relation, Eq. (2), represents the algebraic Lyapunov equation which shows that an SPR system is asymptotically stable, while Eq. (3) shows that $B_p^T (P_p B_p) = B_p^T C_p^T = C_p B_p$. It can also be shown that both relations, Eqs. (2) and (3), imply that the system is strictly minimum-phase. As the SP properties are not inherently satisfied in most real-world systems, a class of almost strictly passive (ASP) systems can be defined through the following definition.[11]

Definition 2: The LTI system described by Eq. (1) with the $m \times m$ transfer function given by $G_p(s) = C_p (sI - A_p)^{-1} B_p$ is almost strictly passive (ASP) and its transfer function almost strictly positive real (ASPR) if there exists a constant fictitious output feedback gain $\tilde{K}_e$ such that the fictitious closed-loop system with the system matrix

$$A_c = A_p - B_p \tilde{K}_e C_p \tag{4}$$

satisfies the Kalman-Yakubovich-Popov conditions

$$PA_c + A_c^T P = -Q \tag{5}$$

$$PB_p = C_p^T \tag{6}$$

It is obvious that Eqs. (5) and (6) are equivalent to the strict positive realness of the fictitious closed-loop system $\{A_c, B_p, C_p, 0\}$. Since the original plant $\{A_p, B_p, C_p, 0\}$ is being separated from strict positive realness by only a constant output feedback, it is thus referred to as ASPR. Over the years, many works have attempted to clearly define what classes of systems satisfied the ASP/ASPR conditions. Although some early results and proofs had been obtained in the Russian literature for both SIMO and MIMO systems (see translations by Fradkov[13]), these basic conditions, despite having been recalled by several authors,[14,15,16] have remained unknown to the control community. Since then, many other works have independently reformulated the ASP/ASPR conditions.[17] See work by Fradkov[18] and Barkana[19] for complete historical surveys on the subject. It is now widely accepted that any strictly proper strictly minimum-phase LTI system described by Eq. (3) with $C_p B_p > 0$ (i.e. positive definite symmetric) is ASP and its transfer function ASPR.[19,20,21] The nonsingular $C_p B_p$ implies that the corresponding transfer function is of relative degree 1, that is, has n poles and $n-1$ zeros in SISO systems[22,23] or n poles and $n-m$ zeros in $m \times m$ MIMO systems.[24,25,26,27,28,29]

III. Simple Adaptive Control

The problem of self-adjusting the gains of a controller using a direct adaptation mechanism in order to obtain the desired closed-loop characteristics, as defined by a reference model, is the idea behind direct model reference adaptive control (MRAC). To mitigate the reference model-plant order matching requirement inherent to most standard adaptation laws, a simple control gains adaptation mechanism known as simple adaptive control (SAC), was introduced by Sobel et al.[30] and further developed by Barkana et al.[31] and Barkana and Kaufman[32] in the context of large structural space systems. This output feedback adaptive control methodology forces the plant, which could be of very large dimension, to track a reference model, without requiring the model to be of the same order as the plant. As opposed to MRAC, the model used in SAC does not necessarily have to reproduce the plant, aside from incorporating the desired input-output behavior of the plant. In fact, this model could be just a first-order pole that performs a satisfactory response to the user command, or a higher order system, just sufficiently high to generate the ideal trajectory.

As it generates the command, this ideal model can also be referred to as command generator and the corresponding technique is in fact closely related to the command generator tracker approach.[33] In the last few decades, the SAC methodology and variations thereof have been used in many successful linear and nonlinear applications, such as nonminimum phase autopilots,[34] atmospheric entry vehicles,[35,36] spacecraft underactuated attitude control,[37] flexible-joint robot manipulators,[38] and flexible structures with collocated and noncollocated sensors.[39]

III.A. Direct Adaptive Control Law

The output of the plant is required to follow the output of a reference model (not necessarily square)

$$\dot{x}_m = A_m x_m + B_m u_m, \qquad y_m = C_m x_m \tag{7}$$

where $u_m \in \mathbb{R}^p$ denotes the model control inputs, that is, the desired plant outputs specified by the user, $x_m \in \mathbb{R}^{n_m}$ and $y_m \in \mathbb{R}^m$ are the model states and outputs, respectively, and A_m, B_m, and C_m are appropriately dimensioned real matrices. To quantify this control objective, an output tracking error denoted by $e_y \in \mathbb{R}^m$, is defined as

$$e_y \triangleq y_m - y_p \tag{8}$$

In addition to this output tracking error signal, the SAC methodology uses all available data about the model by including the model states and inputs in a feedforward configuration, to compute the control law

$$u_p = K_e(t)e_y + K_x(t)x_m + K_u(t)u_m \tag{9}$$

and to update the control gains using the following adaptation mechanism

$$K_e(t) = K_{Pe}(t) + K_{Ie}(t) \tag{10}$$

$$K_x(t) = K_{Px}(t) + K_{Ix}(t) \tag{11}$$

$$K_u(t) = K_{Pu}(t) + K_{Iu}(t) \tag{12}$$

where $K_e(t) \in \mathbb{R}^{m\times m}$ is the time-varying stabilizing control gain matrix, and $K_x(t) \in \mathbb{R}^{m\times n_m}$ and $K_u(t) \in \mathbb{R}^{m\times p}$ are time-varying feedforward control gains that contribute to bringing the output tracking error to zero. Practice shows that both $K_x(t)$ and $K_u(t)$ allow good tracking without requiring unnecessarily large values of the stabilizing gain $K_e(t)$. The proportional components of the control gains in Eqs. (10)-(12) are adapted as

$$K_{Pe}(t) = e_y e_y^T \Gamma_{Pe} \tag{13}$$

$$K_{Px}(t) = e_y x_m^T \Gamma_{Px} \tag{14}$$

$$K_{Pu}(t) = e_y u_m^T \Gamma_{Pu} \tag{15}$$

and the integral components are updated as

$$\dot{K}_{Ie}(t) = e_y e_y^T \Gamma_{Ie} \tag{16}$$

$$\dot{K}_{Ix}(t) = e_y x_m^T \Gamma_{Ix} \tag{17}$$

$$\dot{K}_{Iu}(t) = e_y u_m^T \Gamma_{Iu} \tag{18}$$

While only the integral adaptive control terms are absolutely needed in Eqs. (10)-(12) to guarantee the stability of the direct adaptive control system, adding the proportional adaptive control terms increases the rate of convergence of the adaptive system toward perfect tracking.[11] In Eqs. (13)-(18), $\Gamma_{Pe}, \Gamma_{Ie} \in \mathbb{R}^{m\times m}$,

$\Gamma_{Px}, \Gamma_{Ix} \in \mathbb{R}^{n_m \times n_m}$ and $\Gamma_{Pu}, \Gamma_{Iu} \in \mathbb{R}^{p \times p}$ are positive-definite diagonal matrices that define the rate of adaptation of the control gains.

The adaptive algorithm can be rewritten in the following consice form

$$u_p = K(t)r \tag{19}$$

where $K(t) \in \mathbb{R}^{m \times (m+n_m+p)}$ and $r \in \mathbb{R}^{(m+n_m+p) \times m}$ are respectively defined as

$$K(t) = \begin{bmatrix} K_e(t) & K_x(t) & K_u(t) \end{bmatrix} = K_P(t) + K_I(t) \tag{20}$$

$$r = \begin{bmatrix} e_y^T & x_m^T & u_m^T \end{bmatrix}^T \tag{21}$$

With this representation, $K_P(t), K_I(t) \in \mathbb{R}^{m \times (m+n_m+p)}$ are updated as follows

$$K_P(t) = e_y r^T \Gamma_P \tag{22}$$

$$\dot{K}_I(t) = e_y r^T \Gamma_I \tag{23}$$

where $\Gamma_P, \Gamma_I \in \mathbb{R}^{(m+n_m+p) \times (m+n_m+p)}$ are the resulting adaptation coefficient matrices for the combined gain $K_p(t)$ and $K_I(t)$

$$\Gamma_P = \begin{bmatrix} \Gamma_{Pe} & & \\ & \Gamma_{Px} & \\ & & \Gamma_{Pu} \end{bmatrix} \qquad \Gamma_I = \begin{bmatrix} \Gamma_{Ie} & & \\ & \Gamma_{Ix} & \\ & & \Gamma_{Iu} \end{bmatrix}$$

III.B. Review of Stability

Before applying the SAC algorithm to the plant, one must have a guarantee of closed-loop stability to show that the errors converge and that the control gains are bounded. When the plant tracks the model perfectly, it moves along a bounded ideal state trajectory, denoted by x_p^*. In other words, the ideal plant

$$\dot{x}_p^* = A_p x_p^* + B_p u_p^*, \qquad y_p^* = C_p x_p^* \tag{24}$$

moves along x_p^*, where u_p^* denotes the ideal control input defined by evaluation the control law at $e_y = 0$, that is

$$u_p^* = \tilde{K}_x x_m + \tilde{K}_u u_m \tag{25}$$

To facilitate the analysis, a state error, denoted by $e_x(t) \in \mathbb{R}^n$, is defined as

$$e_x \triangleq x_p^* - x_p \tag{26}$$

Thus Eq. (8) can be rewritten as

$$e_y = C_p x_p^* - C_p x_p = C_p e_x \tag{27}$$

The differential equation of the state error is obtained by time-differentiating Eq. (26), which results in

$$\dot{e}_x = \left(A_p - B_p \tilde{K}_e C_p\right) e_x - B_p \left(K_I(t) - \tilde{K}\right) r - B_p K_P(t) r \tag{28}$$

In Eq. (28), $\tilde{K} \in \mathbb{R}^{m \times (m+n_m+p)}$ is defined as

$$\tilde{K} = \begin{bmatrix} \tilde{K}_e & \tilde{K}_x & \tilde{K}_u \end{bmatrix} \tag{29}$$

where $\tilde{K}_x \in \mathbb{R}^{m \times n_m}$ and $\tilde{K}_u \in \mathbb{R}^{m \times p}$ are constant ideal feedforward control gains. Since it is required to guarantee the stability of the dynamic adaptive gains and the state error, the following quadratic positive-definite Lyapunov function is considered[11]

$$V(t) = e_x^T P e_x + \mathrm{tr}\left[\left(K_I(t) - \tilde{K}\right) \Gamma_I^{-1} \left(K_I(t) - \tilde{K}\right)^T\right] \tag{30}$$

Time-differentiating Eq. (30), and after some algebra and using the ASP properties in Eqs. (5) and (6), results in

$$\dot{V}(t) = -e_x^T Q e_x - 2e_y^T e_y r^T \Gamma_P r < 0 \tag{31}$$

The Lyapunov derivative Eq. (31) only includes the state error e_x and is therefore negative definite in e_x and negative semidefinite in the state-gain space $\{e_x, K_I(t)\}$. Stability of the adaptive system with respect to boundedness is therefore guaranteed from the Lyapunov stability theory, and all state errors (and output errors), as well as adaptive control gains are bounded. Furthermore, LaSalle's invariance principle for non-autonomous systems[11,40,41,42] can be used to demonstrate that $\{e_x, K_I(t)\}$ ultimately reaches the domain defined by $e_x \equiv 0$. Since $e_x \equiv 0$ implies $e_x(t) = 0$ and $e_y(t) = 0$, asymptotic stability of the state and output tracking errors is guaranteed. Note that, as shown in Eq. (31), adding the proportional terms in the adaptation mechanism adds to the negativity of the Lyapunov derivative, thereby increasing the rate of asymptotic convergence.

III.C. Robustness under Non-Ideal Conditions

It is well recognized that to prevent undesirable divergence of the integral time-varying control gain under non-ideal conditions, the basic adaptive algorithm must be suitably modified. One possible modification is the so-called σ-modification, that has been first mentioned in the work of Narendra et al.[43] which studied the effects of disturbance on stability of conventional MRAC systems, and widely popularized in the work of Ioannou and Kokotovic[44,45] and then by Barkana et al.[11,22,46,47] and Narendra and Annaswamy.[48] The first σ-modification for SAC was proposed by Fradkov[24] and Fomin et al.[49] Here, in the context of SAC, the simplest form of σ-modification is adopted (without any need for switching rules or other modifications that may appear in the literature). With this adjustment, the time-varying integral control gain is obtained as

$$\dot{K}_I(t) = e_y r^T \Gamma_I - \sigma K_I(t) \tag{32}$$

where

$$\sigma = \begin{bmatrix} \sigma_e & & \\ & \sigma_x & \\ & & \sigma_u \end{bmatrix} \in \mathbb{R}^{(m+n_m+p)\times(m+n_m+p)}$$

Thus, according to the Lyapunov stability theory and LaSalle's invariance principle, the application of the adaptive control law with the σ-modification results in bounded error tracking stability, as opposed to asymptotic stability. Note that, although it affects the proof of stability, the use of the adaptive control law with the σ-adjustment is preferable in most practical applications. Under ideal conditions and without the σ term, when the integral gain reaches certain values, it has stabilizing effect on the system and the tracking error decreases. However, if the tracking error cannot reach zero due to unknown external perturbations for example, the integral gain will continue to increase and eventually diverge. Even if the adaptive gains stop increasing and divergence does not occur, they may still maintain large values even when such values are not needed any longer. On the other hand, with the σ term, the integral gain increases only when large tracking errors are present and decreases when large gains are no longer necessary, thus fitting the right gain to the right operational conditions. Furthermore, although the proofs of stability only guarantee ultimately bounded errors, they depend on the distance from the ultimate adaptive gains and any set of the unknown ideal gains that could have achieved perfect following. Therefore, although the proofs cannot and do not promise more, in most cases, the ultimate tracking errors may come out to be practically negligible.

IV. Position Feedback Adaptive Control

IV.A. Plant Dynamics

When the relative motion of the two spacecraft is assumed to be in a Keplerian circular orbit, the nonlinear dynamics may be linearized into the well-known Clohessy-Wiltshire (CW) equations of relative motion[5]

$$\ddot{x} - 3n^2 x - 2n\dot{y} = a_x \tag{33}$$

$$\ddot{y} + 2n\dot{x} = a_y \tag{34}$$

$$\ddot{z} + n^2 z = a_z \tag{35}$$

where x, y and $z \in \mathbb{R}$ denote the relative position coordinates defined with respect to a moving coordinate system with its origin centered at the target spacecraft center of mass, $n \in \mathbb{R}$ denotes the orbital mean motion, and a_x, a_y, and $a_z \in \mathbb{R}$ represent the control accelerations. It is well-known that the in-plane motion (x and y) and out-of-plane motion (z) are decoupled, where the latter is an undamped oscillation with the orbital angular velocity, and where the in-plane coupling terms correspond to Coriolis and gravity forces. For proximity operations, these terms may be considered as low frequency and small disturbances to be compensated by the controller and may thus be neglected in the dynamics model. Consequently, a double integrator model, independent for each axis, may be used, as demonstrated by Fehnse.[50] Alternatively, this simplification can be justified whenever the spacecraft are maneuvering on a faster time scale than the orbital mean motion, n. In fact, this can be seen by observing the bode plot of the double integrator superimposed on CW equations and noting that they are identical in frequencies higher than the rate of the orbit n, as shown by Paluszek and Thomas.[51] In view of the above discussion and assuming a relative position feedback only, the plant dynamics can then be modeled by a double integrator model independent for each axis, as follows

$$\frac{y_p(s)}{u_p(s)} = G_p(s) = \frac{1/m}{s^2} \tag{36}$$

where $m \in \mathbb{R}$ denotes the mass of the chaser spacecraft, $y_p(t) \in \mathbb{R}$ represents a single relative position coordinate output (i.e., $x(t)$, $y(t)$, or $z(t)$), and $u_p(t) \in \mathbb{R}$ denotes the related control input force ($F_x(t)$, $F_x(t)$, or $F_x(t) \in \mathbb{R}$).

IV.B. Parallel Feedforward

As discussed previously, the ASPR properties are the main conditions needed for the proofs of stability with SAC. However, in spite of some specific exceptions, most realistic plants are not ASPR. For example, the plant described by Eq. (36) is of relative degree 2 and is therefore not ASPR. As a result, the simple adaptive control law presented in Section II cannot be directly applied to this problem with any stability guarantees. To mitigate this issue, it was shown that various forms of parallel feedforward configurations (PFC) can be used to satisfy the ASPR conditions, thus extending the applicability of SAC to almost all practical applications.[20,34,52,53,54,55,56,57,58] The idea behind PFC is to use the dynamics of a noncausal controller with sufficiently high gain, in a similar way to any LTI controllers designed to stabilize Eq. (36). Specifically, if the plant $G_p(s)$ can be stabilized through a controller denoted $H(s)$, then the inverse $H^{-1}(s)$ used in parallel with the original plant results in an augmented plant $G_a(s) = G_p(s) + H^{-1}(s)$ which is minimum phase and of relative degree one, thereby making $G_a(s)$ ASPR. Let us herein select a PD controller as a simple control law

$$H(s) = K_p\,(1 + s/w) \tag{37}$$

where $w \in \mathbb{R}$ denotes the control gain ratio K_p/K_d of the PD controller. Let use the inverse of this noncausal controller as parallel feedforward around the plant

$$H^{-1}(s) = \frac{K_p^{-1}}{1 + s/w} \tag{38}$$

It must be emphasized that, although now the feedback variable is the augmented output, the variable of interest remains the output of the actual plant. This is a potential weakness of the PFC methodology. Therefore, it is very important to guarantee that the PFC is sufficiently small so the behavior of the actual plant output is very similar to the behavior of the augmented system. To do so, as highlighted by Eq. (38), the gain of $H(s)$ must be sufficiently large such that its inverse, K_p^{-1}, is small. As a result, the contribution of $H^{-1}(s)$ to the augmented output is expected to be negligible relative to that of the actual plant output, such that $y_a(t) \cong y_p(t)$ for all practical purposes, where $y_a(t)$ denotes the output of the augmented plant. A root locus of the plant with proper selection of control gains for $H(s)$ would indeed show that satisfactory behavior

can be obtained by selecting K_p to a sufficiently large value. The control input force to the augmented plant output transfer function is then

$$\frac{y_a(s)}{u_p(s)} = G_a(s) = G_p(s) + H^{-1}(s) = \frac{K_p^{-1}\left\{s^2 + (K_d/m)\,s + (K_p/m)\right\}}{s^2\,(1 + s/w)} \tag{39}$$

Note that, as expected, the augmented plant $G_a(s)$ is minimum phase and of relative degree of one (two zeros and three poles), which makes it ASPR. Therefore, the simple adaptive control law presented in Section III can be applied to this augmented plant while guaranteeing closed-loop stability.

IV.C. Ideal Model

The plant is required to follow the output of a simple second-order model having a transfer function representation of the form

$$\frac{y_m(s)}{u_m(s)} = G_m(s) = \frac{\omega_n^2}{s^2 + 2\zeta\omega_n s + \omega_n^2} \tag{40}$$

where ω_n and ζ denotes the natural frequency and damping ratio of the ideal closed-loop system.

IV.D. Simulation Results

Numerical simulations in MATLAB/Simulink were performed to assess the effectiveness of the proposed control approach. Although the nominal plant dynamics model is not unknown, uncertainties and/or variations in its dynamics (e.g. external perturbation forces) and its parameter (i.e. the mass), make it a rather difficult system to design by any conventional control methodologies. At nominal design conditions, the applied force to relative spacecraft position (along a given axis) transfer function is

$$\frac{y_p(s)}{u_p(s)} = G_{p1}(s) = \frac{0.2326}{s^2} \tag{41}$$

which represents the dynamics model of a 4.3 kg nanosatellite maneuvering in close proximity of another space vehicle. The differential equation associated with the mathematical model of the plant was integrated using a fixed-timestep fifth-order RungeKutta integration scheme. The control parameters were chosen as

$$\Gamma_{Pe} = 10e3, \quad \Gamma_{Px} = 10e2, \quad \Gamma_{Pu} = 25 \times 10e3, \quad \Gamma_{Ie} = 100, \quad \Gamma_{Ix} = \Gamma_{Iu} = 10, \quad \sigma = \begin{bmatrix} 0.01 & & \\ & 0 & \\ & & 0 \end{bmatrix}$$

These control parameters were selected to obtain a satisfactory response when applied to the nominal plant, that is, the nanosatellite with a mass of 4.3 kg described by Eq. (41). The adaptation algorithm was initialized with $K_{Ie} = K_{Ix} = K_{Iu} = 0$ and the integral structure of these adaptive gains was also computed with fixed-time-step fifth-order Runge-Kutta integration scheme. The model was designed to incorporate the ideal input-output behavior described by $\zeta = 0.9$ and $\omega_n = 0.13$. Note that this ideal model is not based on any modeling of the plant. Furthermore, the specific value of ζ and ω_n were determined such that the ideal model provides a settling time similar to that of the following PD benchmark controller which was designed by Nolet[6] to specifically stabilize the nominal plant, i.e. $G_{p1}(s)$

$$C(s) = 0.0171(1 + 10s) \tag{42}$$

Since $C(s)$ was shown to provide satisfactory stabilization and tracking performance, one might use its inverse as the parallel feedforward around the plant. However, it is recalled that the contribution of the parallel feedforward to the augmented output must be negligible relative to the plant output. This can only be achieved if K_p is sufficiently large, which is not the case with Eq. (42). To do so, the inverse of the following high gain PD controller is used as the parallel feedforward

$$H(s) = 200(1 + s/2.5) \tag{43}$$

Although the practical purpose of the adaptive controller is to achieve robust performance under large mass variations, the strongest demonstration consists in varying the mass of the servicer spacecraft. To this end, numerical simulations using a spacecraft with a larger mass were performed as a mean to assess the robustness of the proposed controller to parametric uncertainties in the plant. The plant transfer function under parametric uncertainty is given by

$$\frac{y_p(s)}{u_p(s)} = G_{p2}(s) = \frac{0.1031}{s^2} \tag{44}$$

which represents a 125% increase of the spacecraft mass. In all simulations, the initial relative position and velocity of the servicer with respect to the target spacecraft were set to 0 m and 0 m/s, respectively, that is, in a docking configuration. At 10 sec., the chaser undocks and travels to the desired relative position, which is set to 1 m. In the context of DARPA's Phoenix program, given the initial conditions and the desired relative position, the nominal plant given by Eq. (41) is representative of a scenario where the nanosatellite with a known mass simply undocks from another spacecraft and travels away from it to accomplish any other tasks that might be required by the mission planners, whereas the uncertain plant described by Eq. (44) represents the case where the nanosatellite has retrieved a component of an unknown mass from the de-commisionned spacecraft and is maneuvering 1 m away relative to it.

The obtained results are provided in Figs. 1 and 2 for the benchmark controller $C(s)$ and the adaptive controller, respectively. As illustrated in Fig. 1, although the nominal response is satisfactory with the PD controller, the uncertain situation exhibits a trajectory overshoot. On the other hand, with the adaptive control strategy, the plant responds adequately to the desired input for both cases, with no overshoot, and with the same transient characteristics. This demonstrates the clear improvement in terms of robustness to parametric uncertainties obtained using the adaptive strategy.

For completeness, the robustness to an unknown external perturbation is also assessed for both the nominal and uncertain case. To this end, a perturbation described by

$$u_{per}(t) = 0.01 \sin(0.01t) \tag{45}$$

is added to the control input $u_p(t)$. The undesirable behavior associated with the PD controller is further aggravated, as illustrated by a larger trajectory overshoot and sustained oscillations that fail to converge to the desired steady-state value within an acceptable time period (see Fig. 4), whereas the adaptive controller yields similar responses for both the nominal and uncertain cases regardless of the presence of the unknown external perturbation force (see Fig. 5). As shown in Figs. 3 and 6, the improved behavior obtained with the direct adaptive control strategy is possible because the control gains are adapting such that they can maintain small tracking errors in different unknown situations.

In addition, a closer look at the control input forces for both controllers (shown in Figs. 7 and 8, respectively) reveals that this improvement in performance is not achieved at the cost of increased control effort. In fact, because the PD controller feeds back the error between the desired input and the actual position and velocity, the initial positioning tracking error at 10 sec. peaks instantaneously to 1 m causing the derivative of this error to be even larger. In turn, the required control force peaks to a high value at 10 sec., on the order of 172 N for all four PD simulation cases. As demonstrated in Fig. 8, such an undesirable behavior is less important with the adaptive controller since it feeds back the tracking error defined with respect to the output of the reference model, which is a smooth trajectory as opposed to a sharp step command input. However, although the control input force peaks to 0.1892 and 0.0814 N for the nominal and uncertain case with no external perturbation, this signal nevertheless peaks to 1.2427 and 7.5734 N for the nominal and uncertain case with the unknown external perturbation. While this is a significant improvement compared to the PD controller performance, this is considered to be relatively high, especially for such a small space vehicle. The reason for this high control input can be explained by the undamped oscillating mode of the plant dynamics which represents a difficult case to be stabilized by any position feedback controllers (including adaptive controllers). The required damping effect which is not included in the adaptive control law is achieved through a large control input signal. In turn, this may prohibit the use of this adaptive control strategy for practical situations where the control input is saturated to a given value, as imposed by the actual actuators employed.

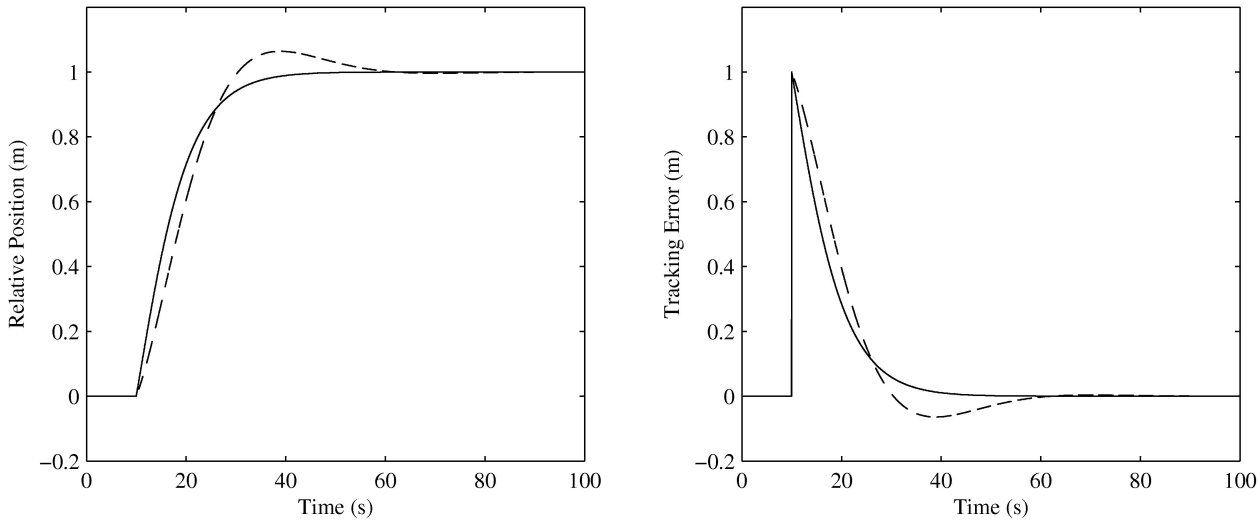

Figure 1. Plant response obtained with the PD controller $C(s)$. The solid lines correspond to the nominal case, and the dashed lines to the uncertain case.

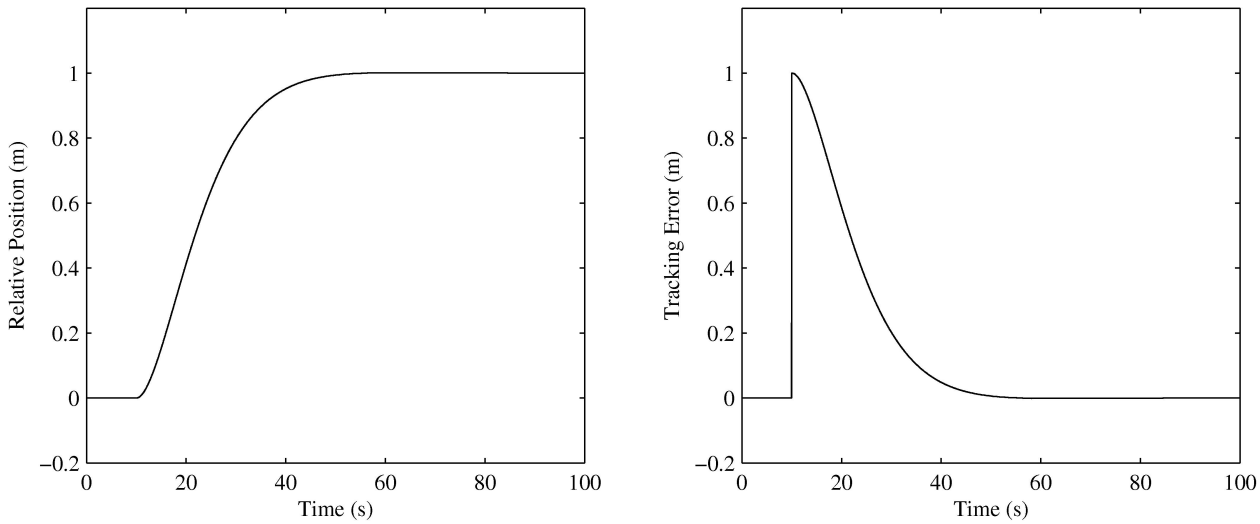

Figure 2. Plant response obtained with the position feedback adaptive controller. The solid lines correspond to the nominal case, and the dashed lines to the uncertain case (almost identical to the nominal case).

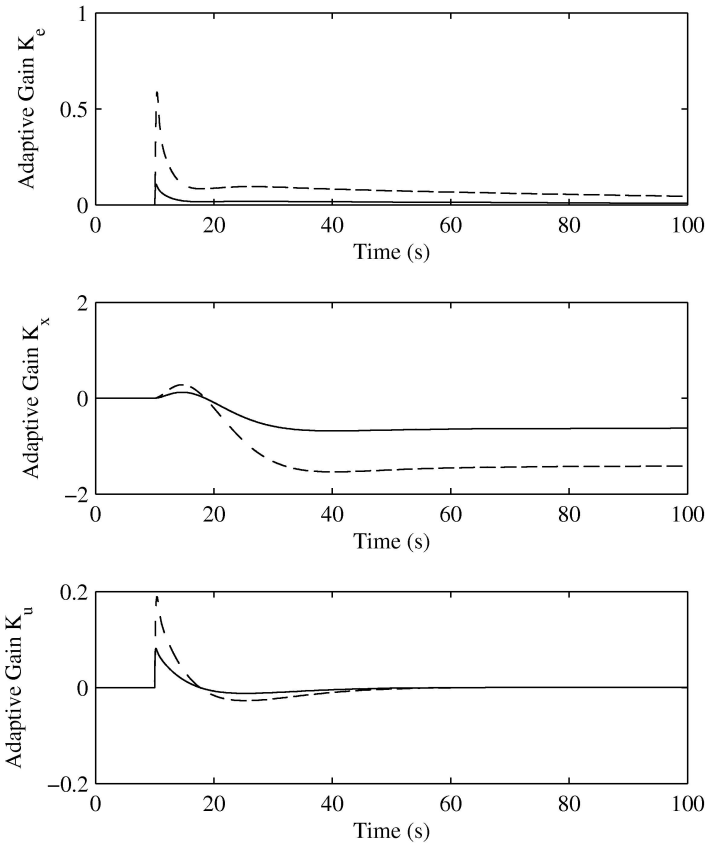

Figure 3. Control gains adaptation history of the position feedback adaptive controller. The solid lines correspond to the nominal case, and the dashed lines to the uncertain case.

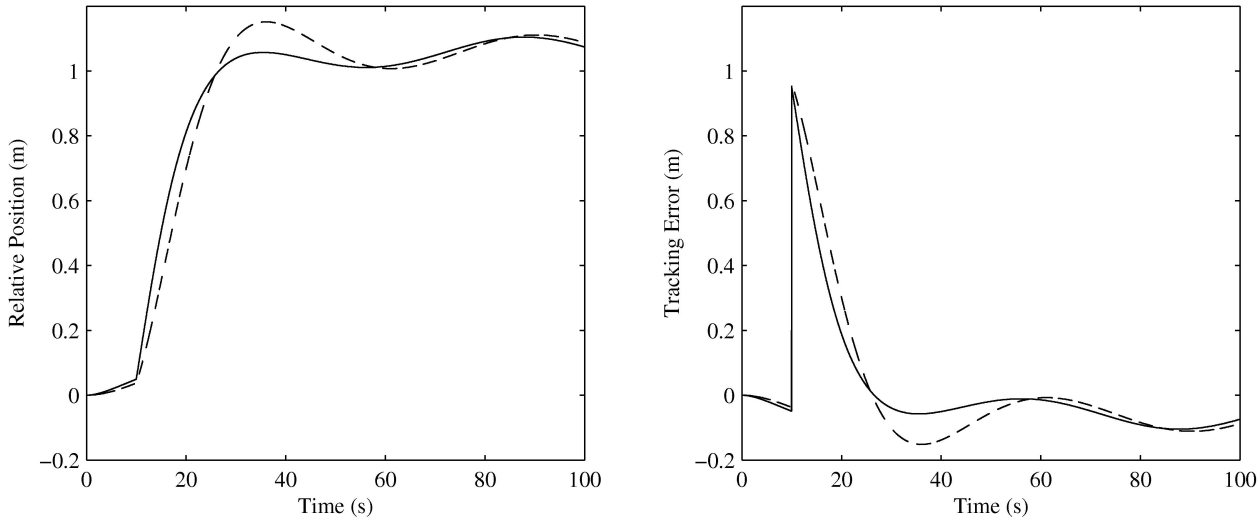

Figure 4. Plant response obtained with the PD controller $C(s)$ under the unknown perturbation. The solid lines correspond to the nominal case, and the dashed lines to the uncertain case.

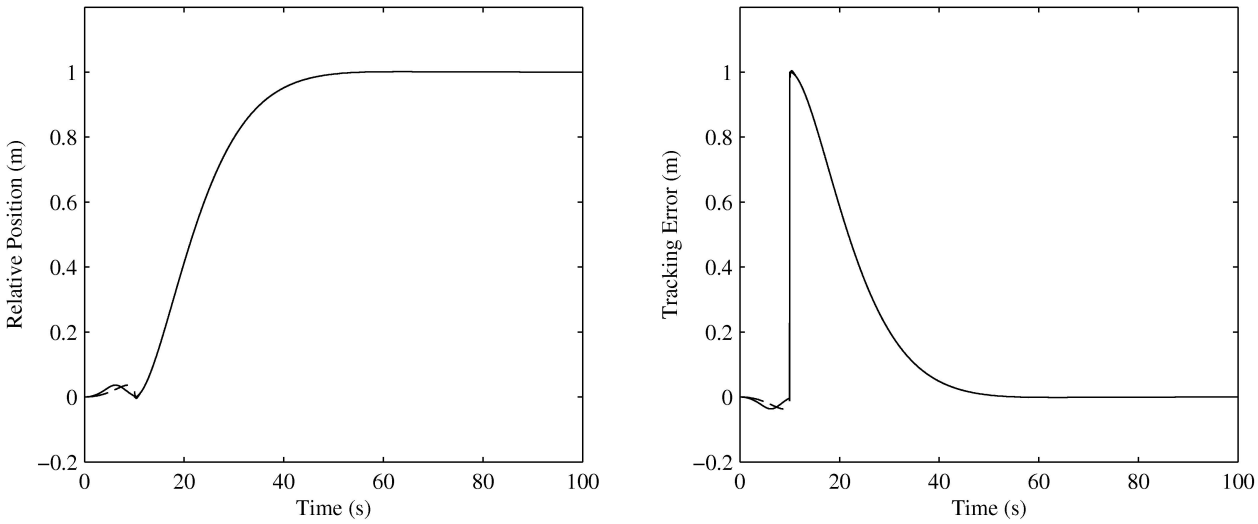

Figure 5. Plant response obtained with the position feedback adaptive controller under the unknown perturbation. The solid lines correspond to the nominal case, and the dashed lines to the uncertain case (almost identical to the nominal case).

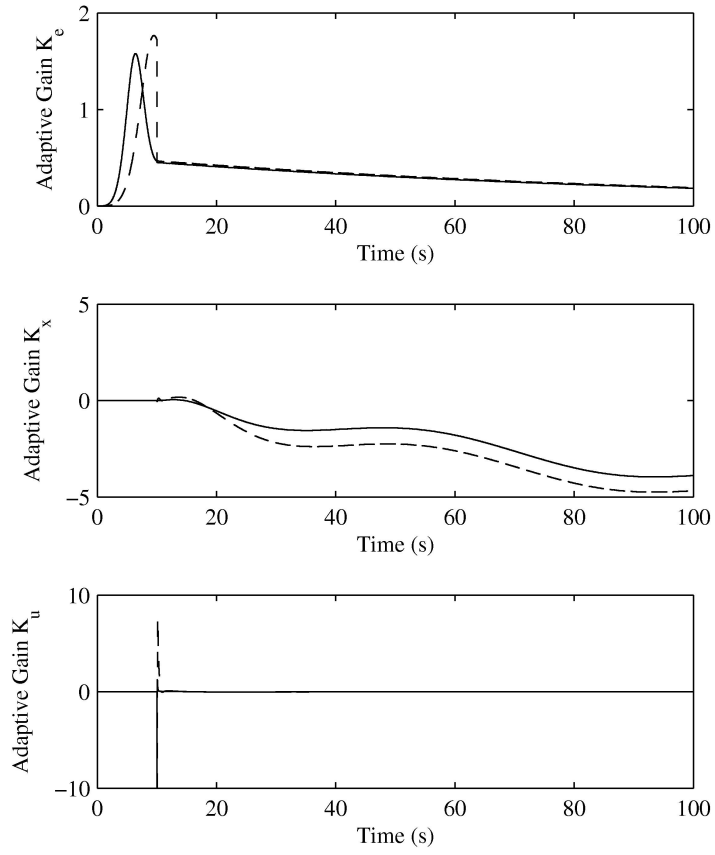

Figure 6. Control gains adaptation history of the position feedback adaptive controller under the unknown perturbation. The solid lines correspond to the nominal case, and the dashed lines to the uncertain case.

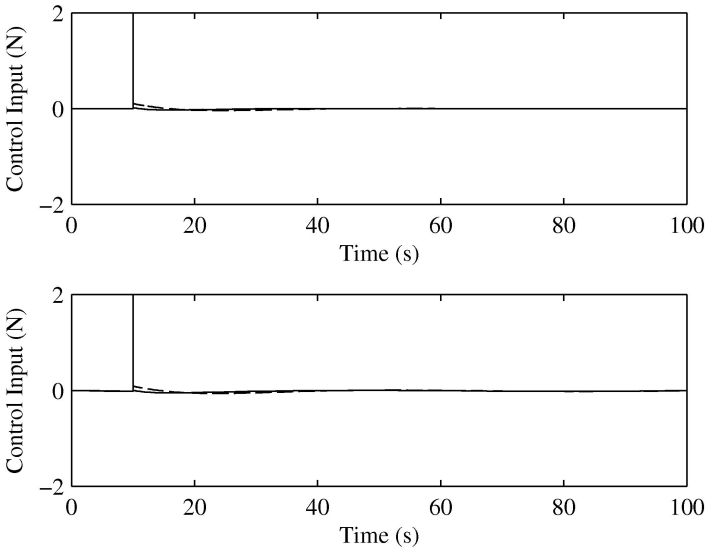

Figure 7. Control input force $u_p(t)$ for the PD controller. Top figure is with no external perturbation, and bottom figure is with the unknown external perturbation. The solid lines correspond to the nominal case, and the dashed lines to the uncertain case.

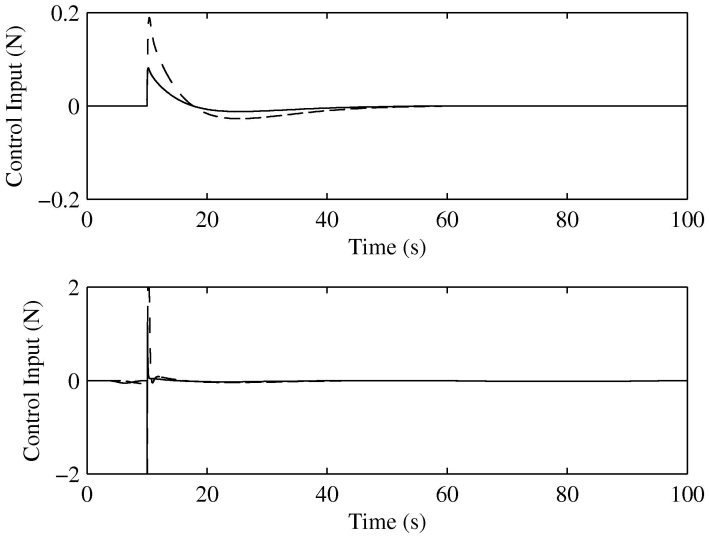

Figure 8. Control input force $u_p(t)$ for the position feedback adaptive controller. Top figure is with no external perturbation, and bottom figure is with the unknown external perturbation. The solid lines correspond to the nominal case, and the dashed lines to the uncertain case.

V. Position-Plus-Velocity Feedback Adaptive Control

One possible solution to add damping to the system would be to use a velocity-only feedback control law. However, even if the feasibility and associated proof of stability of a velocity feedback controller can be derived, position rather than velocity control is what one is interested in. To this end, it will be shown in this section how the use of position along with velocity feedback in a combined single output can significantly improve the performance while still guaranteeing closed-loop stability through the satisfaction of the ASP/ASPR conditions.

V.A. Plant Dynamics

Assuming both the relative position and velocity, denoted by $y_{p1}(t)$ and $y_{p2}(t)$ respectively, can be measured, a combined position-plus-velocity output of the form $y_p(t) = \alpha y_{p1}(t) + y_{p2}(t)$ can be defined. As one does not require the states for the feedback control law, that is, the position or velocity are not required separately, the plant can simply be modeled as a transfer function of the form

$$\frac{y_p(s)}{u_p(s)} = G_p(s) = \frac{1/m(s+\alpha)}{s^2} \tag{46}$$

where α denotes the positive-definite ratio of position to velocity output. It is then easy to see that besides being of relative degree one, the transfer function of the plant given by Eq. (46) is also minimum phase. As a result, $G_p(s)$ is ASPR, thus satisfying the sufficient condition for closed-loop stability required for the application of SAC. Note that since Eq. (46) is of relative degree one, a parallel feedforward configuration is not required anymore.

V.B. Ideal Model

The previously designed ideal model given by Eq. (40) is now redefined such that its output corresponds to a scaled position-plus-velocity signal. Specifically, the model is represented as a state-space formulation described by Eq. (7) with matrices

$$A_m = \begin{bmatrix} 0 & 1 \\ -\omega_n^2 & -2\zeta\omega_n \end{bmatrix}, \qquad B_m = \begin{bmatrix} 0 \\ \omega_n^2 \end{bmatrix}, \qquad C_m = \begin{bmatrix} \alpha C_{m1} & C_{m2} \end{bmatrix}$$

and with

$$x_m = \begin{bmatrix} x_{m1} \\ x_{m2} \end{bmatrix}, \qquad y_m = \alpha y_{m1} + y_{m2}, \qquad y_{m1} = C_{m1} x_{m1}, \qquad y_{m2} = C_{m2} x_{m2}$$

where x_{m1} and x_{m2} denote, respectively the relative position and velocity of the ideal model, i.e., the ideal relative position and velocity of the closed-loop system.

V.C. Simulation Results

As in the previous section, the position-plus-velocity feedback control strategy was validated in numerical simulations for four different cases: 1) with the nominal plant Eq. (46) with a mass of 4.3 kg, 2) with the uncertain plant defined with a mass of 9.7 kg, 3) with the nominal plant and with the unknown external perturbation given by Eq. (45), and finally 4) with the uncertain plant and the unknown perturbation. The position-plus-velocity adaptive feedback control law was designed with

$$\Gamma_{Pe} = 10e5, \quad \Gamma_{Px} = 20, \quad \Gamma_{Pu} = 20, \quad \Gamma_{Ie} = 5, \quad \Gamma_{Ix} = I_2, \quad \Gamma_{Iu} = 1$$

$$\sigma_e = 0.01, \quad \sigma_x = \sigma_u = 0$$

The adaptation algorithm was activated with $K_{Ie} = K_{Iu} = 0$ and $K_{Ix} = \begin{bmatrix} 0 & 0 \end{bmatrix}$. The parameters of the reference model were selected as $C_{m1} = C_{m2} = 1$, and to provide the same transient characteristics as before, i.e., with $\zeta = 0.9$ and $\omega_n = 0.13$. For both the plant and the reference model, the ratio of position to velocity output, α, was set to 0.1.

The tracking results are shown in Figs. 9 and 11. As demonstrated in these figures, the plant exhibits a satisfactory tracking performance, with a similar response in all cases. It is recalled that since the adaptive controller parameters were tuned to provide good results with the nominal dynamics, the obtained results clearly indicate that the adaptive controller is robust to the large parametric uncertainty and to the unknown external force acting on the plant. Indeed, these tuning parameters were kept the same for all cases. As expected, such a good performance is attributable to the control gains, which are adapted in real-time according to the actual tracking situation to provide efficient tracking of the reference model output, regardless of uncertainties and unknown dynamics. In other words, as with the position feedback adaptive controller, this is due to the controller gains that are adapted to force the actual plant to behave as closely as possible to the ideal model (see Figs. 10 and 12). Furthermore, as expected, additional damping into the control law through the combined position-plus-velocity output feedback of the form $\alpha y_{p1} + y_{p2}$ greatly reduces the required control effort, as depicted in Fig. 13.

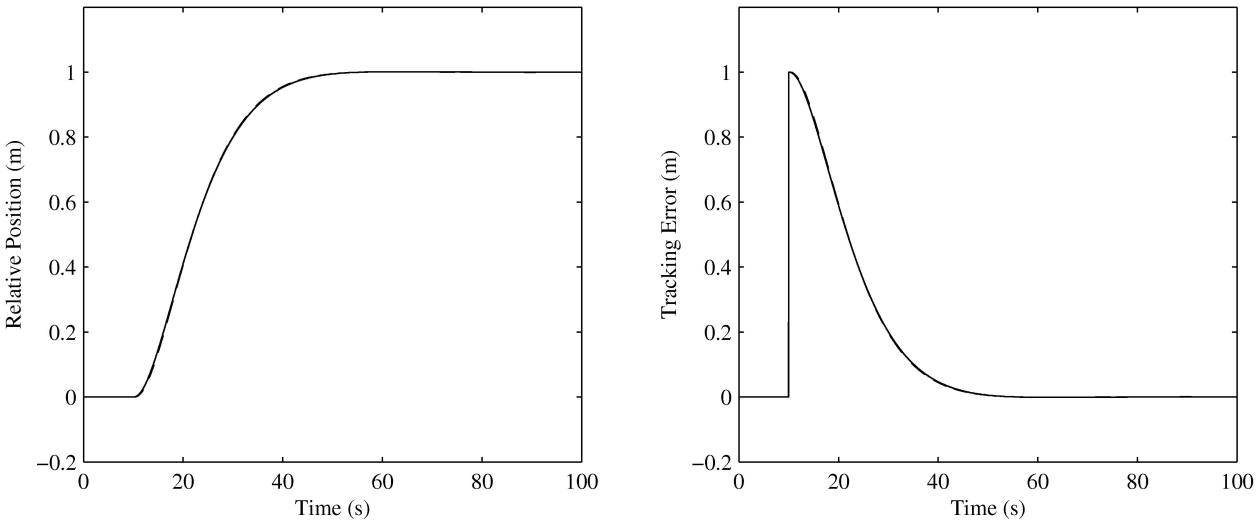

Figure 9. Plant response obtained with the position-plus-velocity feedback adaptive controller. The solid lines correspond to the nominal case, and the dashed lines to the uncertain case (almost identical to the nominal case).

VI. Experimental Results

To demonstrate the applicability of the position-plus-velocity adaptive control law to realistic space systems with limited computational resources, an experiment with the Synchronized Position Hold Engage Reorient Experimental Satellites (SPHERES) air bearing flat floor facility at the MIT Space Systems Laboratory was performed. SPHERES is an experimental testbed consisting of a group of small vehicles with the basic functionalities of a realistic nanosatellite that maneuvers using CO_2 thrusters. Their inertial positioning system is based an extended Kalman filter (EKF) that calculates an estimate of the states based on measurements obtained from an inertial measurement unit (IMU) at 20 Hz and from the time of flight of ultrasound pulses generated at 5 Hz by beacons located at known positions within the test volume.[59] Each spacecraft is programmed in C code via the Texas Instruments Code Composer Studio integrated development environment (IDE). This IDE provides the interfaces to the C6701 digital signal processing (DSP) unit used aboard the nanosatellites. The interfaces include access to real-time threads for estimation, and control. However, the DSP has limited processing capabilities, as it operates at 167 MHz, has 16MB of RAM, and

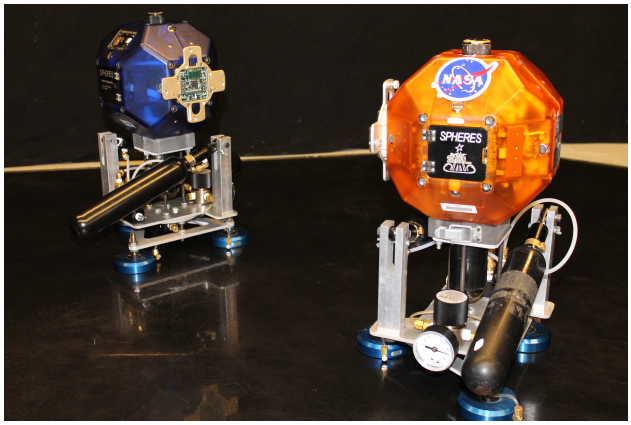

Figure 14. Picture of two SPHERES operating in close proximity at the MIT Space Systems Laboratory.

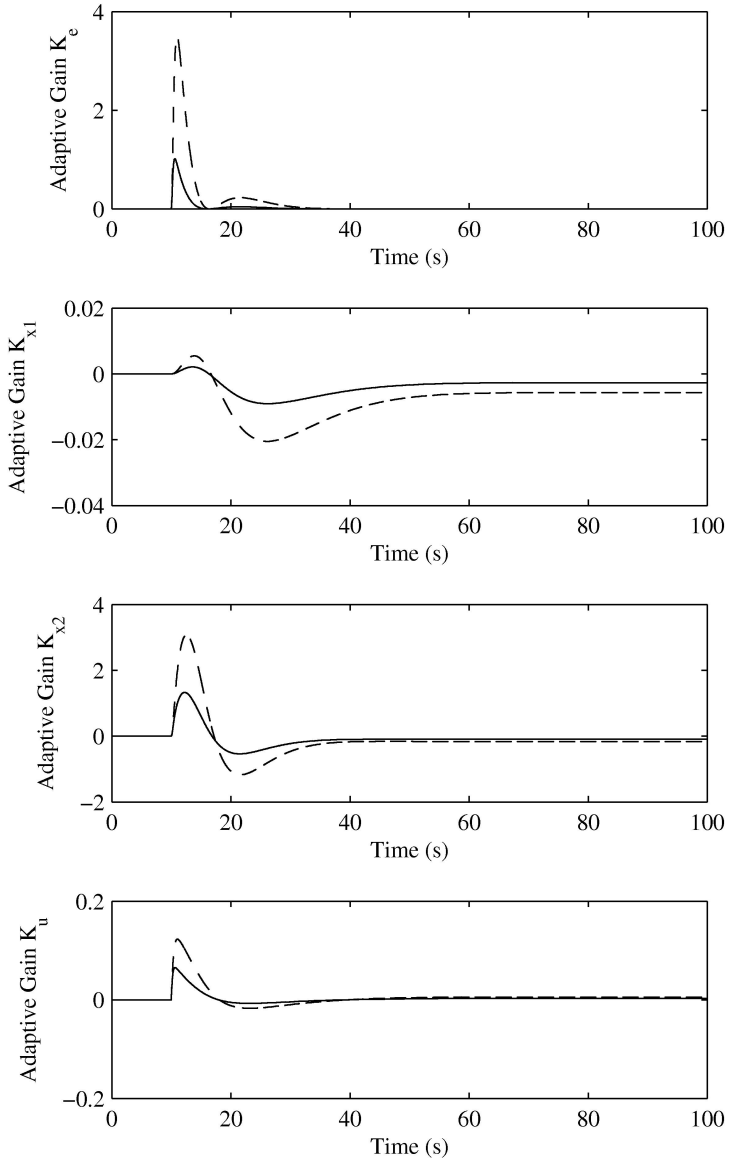

Figure 10. Control gains adaptation history of the position-plus-velocity feedback adaptive controller. The solid lines correspond to the nominal case, and the dashed lines to the uncertain case.

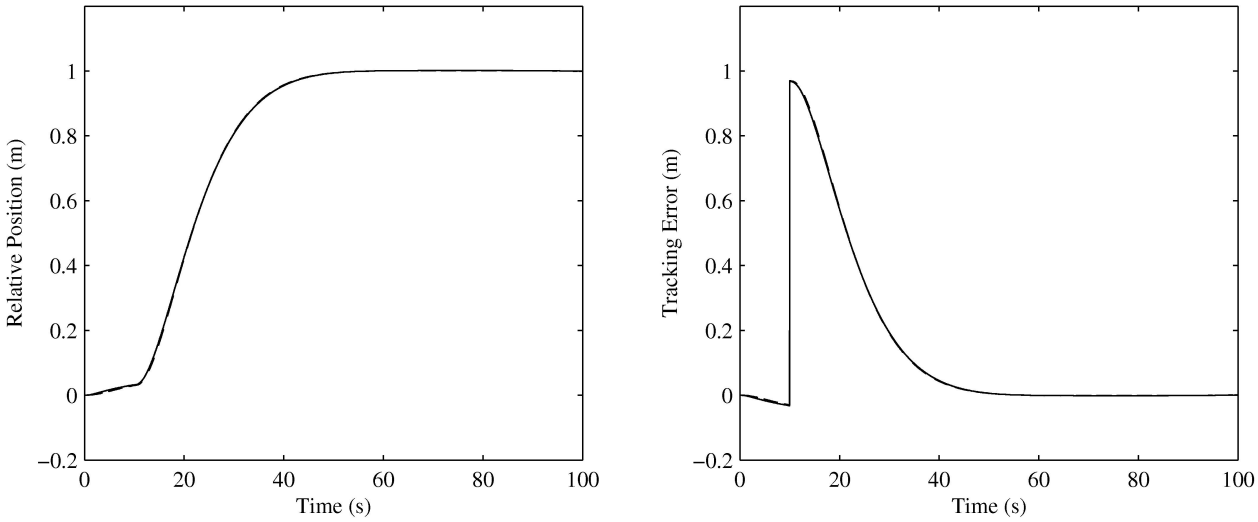

Figure 11. Plant response obtained with the position-plus-velocity feedback adaptive controller under the unknown perturbation. The solid lines correspond to the nominal case, and the dashed lines to the uncertain case (almost identical to the nominal case).

256k of available FLASH. Figure 14 shows a picture of the testbed used for the experiment conducted in this work.

The maneuver used for the experiment is the same as described before, that is, an undocking maneuver where both satellites are initially at rest, and then the servicer spacecraft undocks from the client spacecraft and travel 1 m away from it. During the experiment, the target vehicle is kept fixed. For the experiment, only the uncertain case could be tested as both SPHERES had to be installed on air carriages to provide them with a floating capability on the epoxy flat floor, thereby increasing their nominal mass of 4.3 kg to about 9.7 kg. However, as for the simulation tests described in the previous sections, the control parameters were selected to provide satisfactory performance for the nominal case in a high fidelity numerical simulation. This way, the robustness of the adaptive control law to a mass uncertainty can be validated. The high fidelity numerical simulation consists in a C/C++ environment that models the actual hardware components of the satellites (actuators, sensors, multiple thread computing, limited available computing power, time delays, noise, etc.).

Figures 15 to 19 report the results of the experimental test, which lasted 113 seconds. During the first 10 seconds, both vehicles are at rest, in a docking configuration. During that time, the extended Kalman filter converges to a solution. At 10 seconds into the experiment, the vehicle begins to maneuver through autonomous control by opening the solenoid valves regulating the air flow to the thrusters of the chaser vehicle. As demonstrated in Fig. 15 and 16, better tracking performance under parametric uncertainties is achieved by the position-plus-velocity adaptive control law compared to the PD controller. This is illustrated in Figs. 15 and 16 by a maximum trajectory overshoot at 45 seconds of 0.20 m for the PD control law compared to 0.02 m for the direct adaptive control law. This increased in performance is attributable to the time-varying control gains shown in Fig. 17 which adapt to the current tracking situation, and reached appropriate values at any given time to maintain the trajectory tracking performance under adverse conditions. As expected, and as demonstrated by the results, the constant control gain strategy does not provide a satisfactory response, since the gains were tuned for the nominal, lower mass, case. Indeed, to achieve good results when the mass of the plant is significantly increased, the gains must be tuned such that larger control input forces are applied to the plant. This is shown in Figs. 18 and 19 where the resulting control input force for the PD controller reaches lower values compared to that obtained with the adaptive controller. In turn, the low PD control input force does not prove to be adequate to control the relative position of the satellite. Similar to the simulation results obtained in the previous sections, a sharp and sudden increase in the PD control input signal at 10 seconds into the experiment can be observed, whereas a smoother control input response is obtained with the adaptive controller.

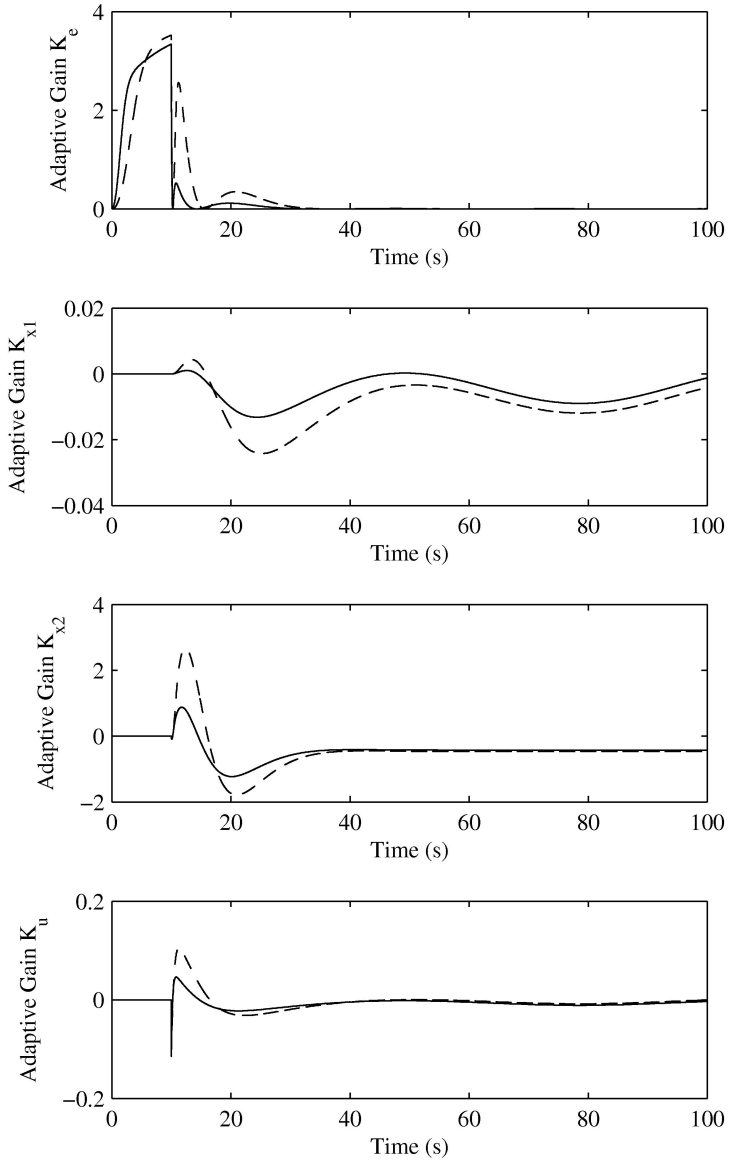

Figure 12. Control gains adaptation history of the position-plus-velocity feedback adaptive controller under the unknown perturbation. The solid lines correspond to the nominal case, and the dashed lines to the uncertain case.

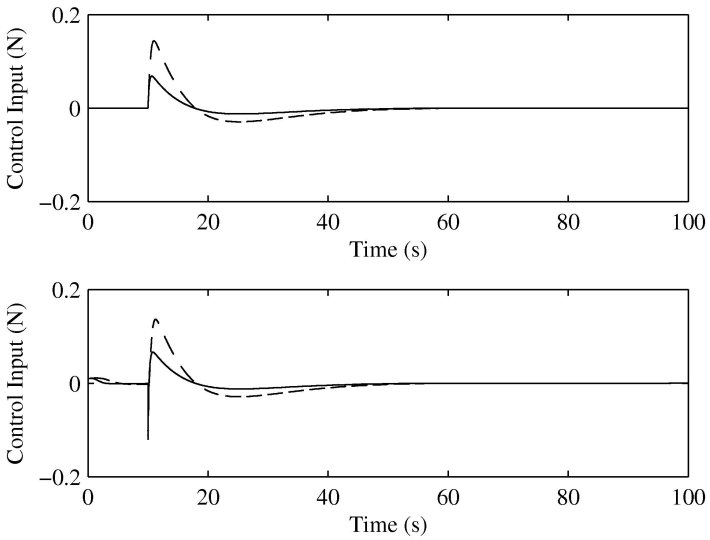

Figure 13. Control input force $u_p(t)$ for the position-plus-velocity feedback adaptive controller. Top figure is with no external perturbation, and bottom figure is with the unknown external perturbation. The solid lines correspond to the nominal case, and the dashed lines to the uncertain case.

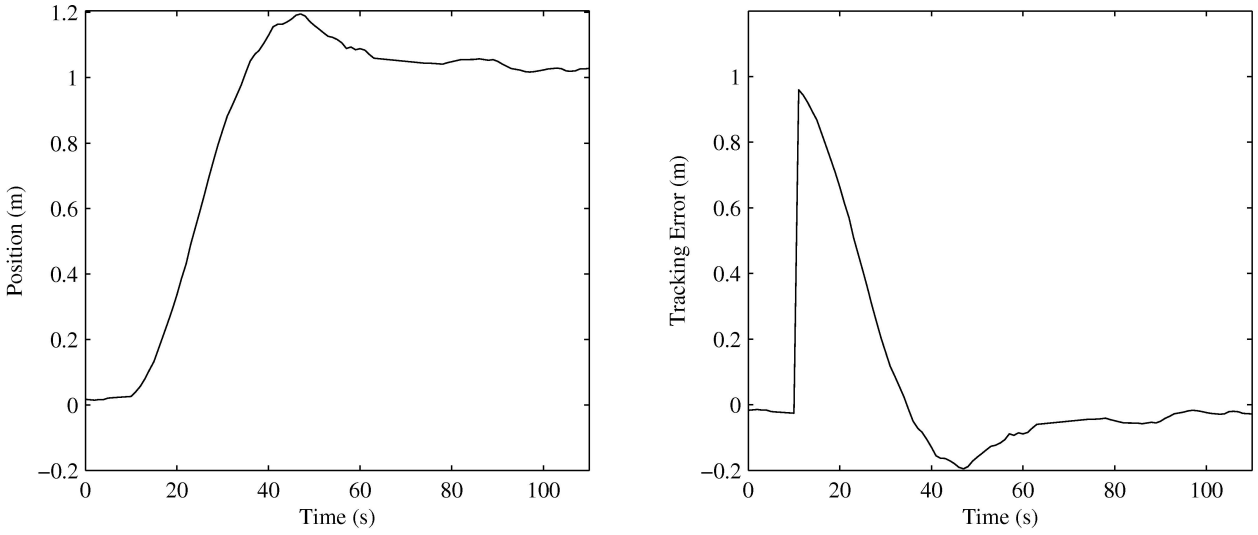

Figure 15. Experimental response obtained with the PD controller $C(s)$ under parametric uncertainties.

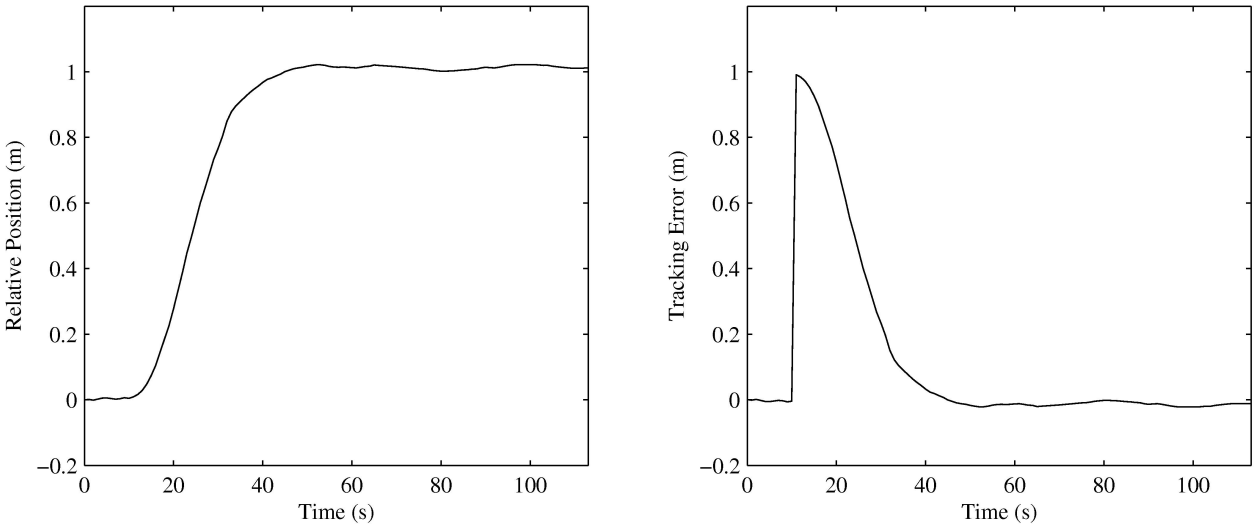

Figure 16. Experimental response obtained with the position-plus-velocity feedback adaptive controller under parametric uncertainties.

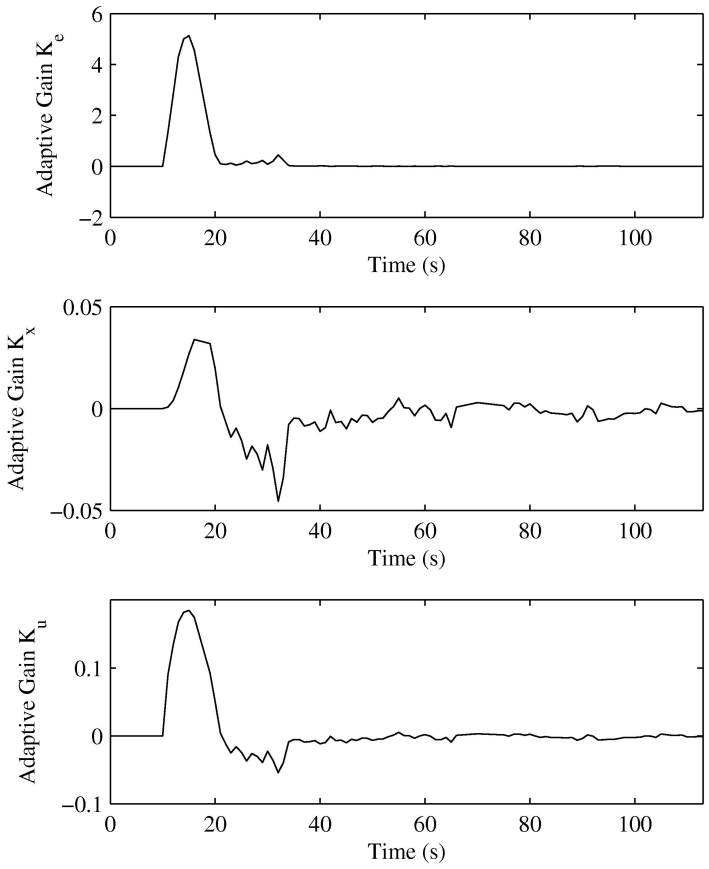

Figure 17. Experimental control gains adaptation history of the position-plus-velocity feedback adaptive controller under parametric uncertainties. The solid lines correspond to the nominal case, and the dashed lines to the uncertain case.

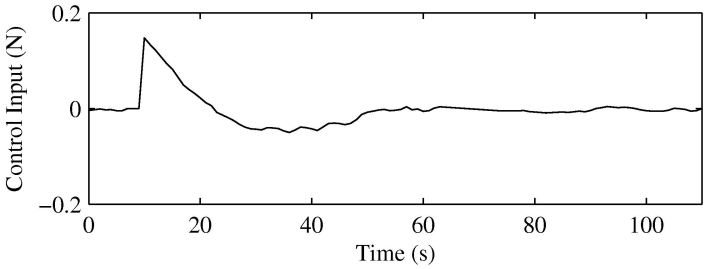

Figure 18. Experimental control input force $u_p(t)$ for the PD controller under parametric uncertainties.

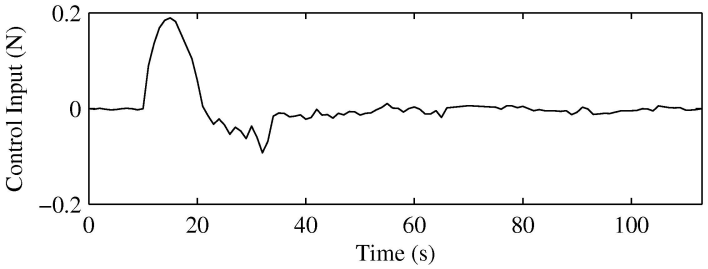

Figure 19. Experimental control input force $u_p(t)$ for the position-plus-velocity feedback adaptive controller under parametric uncertainties.

VII. Conclusion

This paper addressed the problem of adaptive trajectory tracking control for spacecraft close proximity operations under a mass uncertainty and an unknown external perturbation. Based on the simple adaptive control theory, an adaptive control law was developed using a position feedback and a parallel feedforward configuration around the plant in order to satisfy the sufficient almost strictly positive conditions required to guarantee closed-loop stability. While this controller was found to yield superior tracking results and improved robustness over a standard PD controller, its applicability to a practical situation was found to be restrictive. Then, a second adaptive control strategy was derived using a position-plus-velocity feedback, which was found to satisfy the necessary conditions for stability without requiring the additional parallel feedforward configuration. When evaluated in numerical simulations, this latter strategy also demonstrated improved tracking results and robustness under adverse conditions compared to the PD controller. Combined with the simplicity of this control law, this robustness characteristic makes this controller particularly well suited for real-time implementation onboard a spacecraft with limited computing power, as demonstrated with experiments performed with the Synchronized Position Hold Engage Reorient Experimental Satellites facility at the Massachusetts Institute of Technology's Space Systems Laboratory.

Acknowledgments

This work was supported in part by the Natural Sciences and Engineering Research Council of Canada (NSERC) under the Postdoctorate Fellowship Award PDF-438572-2013.

References

[1]Geller, D. K., "Orbital Rendezvous: When is Autonomy Required," *Journal of Guidance, Control, and Dynamics*, Vol. 30, No. 4, 2007, pp. 974–981.

[2]Woffinden, D. C. and Geller, D. K., "Navigating the Road to Autonomous Orbital Rendezvous," *Journal of Spacecraft and Rockets*, Vol. 44, No. 4, 2007, pp. 898–909.

[3]Weismuller, T. and Leinz, M., "GN&C Technology Demonstrated by the Orbital Express Autonomous Rendezvous and Capture Sensor System," *29th Annual AAS Guidance and Control Conference*, Breckenridge, CO, 2006, AAS paper 06-016.

[4]Kremer, A. E., "Russian Craft Has Glitch in Docking with Space Station," *The New York Times*, 24 July, 2012.

[5]Clohessy, W. H. and Wiltshire, R. S., "Terminal Guidance System for Satellite Rendezvous," *Journal of the Aerospace Sciences*, Vol. 27, No. 9, 1960, pp. 653–658.

[6]Nolet, S., *Development of a Guidance, Navigation and Control Architecture and validation Process Enabling Autonomous*

Docking to a Tumbling Satellite, Ph.D. thesis, Massachusetts Institute of Technology, Department of Aeronautics and Astronautics, Cambridge, MA, 2007.

[7]Fezjic, A., *Development of Control and Autonomy Algorithms for Docking to Complex Tumbling Satellites*, Master's thesis, Massachusetts Institute of Technology, Department of Aeronautics and Astronautics, Cambridge, MA, 2008.

[8]Yang, X., Bo, Y., Liu, Y., Jiand, Z., and Gao, H., "Output Tracking Control for Autonomous Spacecraft Rendezvous," *48th IEEE Conference on Decision and Control*, Inst. of Electrical and Electronics Engineers, 2009.

[9]Egardt, B., *Stability of Adaptive Controllers*, Springler-Verlag, Berlin, 1979.

[10]Singla, P., Subbarao, K., and Junkins, J. L., "Adaptive Output Feedback Control for Spacecraft Rendezvous and Docking Under Measurement Uncertainty," *Journal of Guidance, Control, and Dynamics*, Vol. 29, No. 4, 2006, pp. 892–902.

[11]Kaufman, H., Barkana, I., and Sobel, K., *Direct Adaptive Control Algorithms: Theory and Applications*, Communications and Control Engineering Series, Springler, New York, NY, 2nd ed., 1997.

[12]Anderson, B. D. O. and Vongpanitlerd, S., *Network Analysis and Synthesis*, PrenticeHall, Englewood Cliffs, NJ, 1973.

[13]Fradkov, A. L., "Synthesis of an Adaptive System for Linear Plant Stabilization," *Automation and Remote Control*, Vol. 35, No. 12, 1974, pp. 1960–1966.

[14]Andrievsky, B. R., Churilov, A. N., and Fradkov, A. L., "Feedback Kalman-Yakubovich Lemma and its Applications to Adaptive Control," *35th IEEE Conference on Decision and Control*, Inst. of Electrical and Electronics Engineers, 1996.

[15]Andrievsky, B. R., Fradkov, A. L., and Kaufman, H., "Necessary and Sufficient Conditions for Almost Strict Positive Realness and their Application to Direct Implicit Adaptive Control Systems," *American Control Conference*, Baltimore, MD, 1994, pp. 1265–1266.

[16]Fradkov, A. L. and Hill, D. J., "Exponential Feedback Passivity and Stabilizability of Nonlinear Systems," *Automatica*, Vol. 34, No. 6, 1998, pp. 697–703.

[17]Huang, C.-H., Ioannou, P. A., Maroulas, J., and Safonov, M. G., "Design of Strictly Positive Real Systems using Constant Output Feedback," *IEEE Transactions on Automatic Control*, Vol. 44, No. 3, 1999, pp. 569–573.

[18]Fradkov, A. L., "Passification of Non-square Linear Systems and Feedback Yakubovich-Kalman-Popov Lemma," *European Journal of Control*, Vol. 9, No. 6, 2003, pp. 573–582.

[19]Barkana, I., "Comments on Design of Strictly Positive Real Systems Using Constant Output Feedback," *IEEE Transactions on Automatic Control*, Vol. 49, No. 11, 2004, pp. 2091–2093.

[20]Weiss, H., Wang, Q., and Speyer, J. L., "System Characterization of Positive Real Conditions," *IEEE Transactions on Automatic Control*, Vol. 39, No. 3, 1994, pp. 540–544.

[21]Barkana, I., "Positive Realness in Multivariable Stationary Linear Systems," *Journal of the Franklin Institute*, Vol. 328, No. 4, 1991, pp. 403–417.

[22]Barkana, I., "Parallel Feedforward and Simplified Adaptive Control," *International Journal of Adaptive Control and Signal Processing*, Vol. 1, No. 2, 1987, pp. 95–109.

[23]Steinberg, A., "A Sufficient Condition for Output Feedback Stabilization of Uncertain Dynamical Systems," *IEEE Transactions on Automatic Control*, Vol. 33, No. 7, 1988, pp. 676–677.

[24]Fradkov, A. L., "Quadratic Lyapunov Function in the Adaptive Stabilization Problem of a Linear Dynamic Plant," *Siberian Mathematical Journal*, Vol. 17, No. 2, 1976, pp. 341–348.

[25]Owens, D. H., Prazel-Walters, D., and Ilchmann, A., "Positive-Real Structure and High-Gain Adaptive Stabilization," *IMA Journal of Mathematical Control and Information*, Vol. 4, No. 2, 1987, pp. 167–181.

[26]Teixeira, M. C. M., *Real Positive Systems and Adaptive Control*, Ph.D. thesis, Pontificia Universidade Catolica, Rio de Janeiro, Brazil, 1989.

[27]Teixeira, M. C. M., "On Strictly Positive Real Matrices," Tech. rep., Pontificia Universidade Catolica, 1988.

[28]Gu, G., "Stabilizability Conditions of Multivariable Uncertain Systems via Output Feedback Control," *IEEE Transactions on Automatic Control*, Vol. 35, No. 8, 1990, pp. 925–927.

[29]Huang, C.-H., Ioannou, P. A., Maroulas, J., and Safonov, M. G., "Design of Strictly Positive Real Systems Using Constant Output Feedback," *IEEE Transactions on Automatic Control*, Vol. 44, No. 3, 1999, pp. 569–573.

[30]Sobel, K., Kaufman, H., and Mabius, L., "Implicit Adaptive Control for a Class of MIMO Systems," *IEEE Transactions on Aerospace and Electronic Systems*, Vol. 18, No. 5, 1982, pp. 576–589.

[31]Barkana, I., Kaufman, H., and Balas, M., "Model Reference Adaptive Control of Large Structural Systems," *Journal of Guidance, Control, and Dynamics*, Vol. 6, No. 2, 1983, pp. 112–118.

[32]Barkana, I. and Kaufman, H., "Some Applications of Direct Adaptive Control to Large Structural Systems," *Journal of Guidance, Control, and Dynamics*, Vol. 7, No. 6, 1984, pp. 717–724.

[33]Broussard, J., "Command Generator Tracking," Tech. Rep. TIM-612-3, The Analytical Sciences Corporation.

[34]Barkana, I., "Classical and Simple Adaptive Control for Nonminimum Phase Autopilot Design," *Journal of Guidance, Control, and Dynamics*, Vol. 28, No. 4, 2005, pp. 631–638.

[35]Mooij, E., "Numerical Investigation of Model Reference Adaptive Control for Hypersonic Aircraft," *Journal of Guidance, Control, and Dynamics*, Vol. 24, No. 2, 2001, pp. 315–323.

[36]Ulrich, S. and de Lafontaine, J., "Autonomous Atmospheric Entry on Mars: Performance Improvement using a Novel Adaptive Control Algorithm," *The Journal of the Astronautical Sciences*, Vol. 55, No. 4, 2007, pp. 431–449.

[37]Lam, Q. M. and Barkana, I., "Direct Adaptive Control Treatment to Loss of Attitude Control Actuators," *AIAA Guidance, Navigation, and Control Conference and Exhibit*, Hilton Head, SC, 2007, AIAA paper 2007-6435.

[38]Ulrich, S., Sasiadek, J. Z., and Barkana, I., "Modeling and Direct Adaptive Control of a Flexible-Joint Manipulator," *Journal of Guidance, Control, and Dynamics*, Vol. 35, No. 1, 2012, pp. 25–39.

[39]Barkana, I. and Ben-Asher, J. Z., "Simple Adaptive Control Applications to Large Flexible Structures," *Journal of Guidance, Control, and Dynamics*, Vol. 34, No. 6, 2011, pp. 1929–1932.

[40]LaSalle, J. P., "Stability of Non-Autonomous Systems," *Nonlinear Analysis: Theory, Methods & Applications*, Vol. 1, No. 1, 1976, pp. 83–90.

[41]LaSalle, J. P., *The Stability of Dynamical Systems*, SIAM, New York, NY, 2nd ed., 1976.

[42]Barkana, I., "Simple Adaptive Control - A Stable Direct Model Reference Adaptive Control Methodology - Brief Survey," in press.

[43]Narendra, K. S., Tripathi, S. S., Luders, G., and Kudva, P., Tech. Rep. CT-43, Yale University.

[44]Ioannou, P. A. and Kokotovic, P., *Adaptive Systems with Reduced Models*, Springer-Verlag, New York, NY, 1983.

[45]Ioannou, P. A. and Kokotovic, P., "Instability Analysis and Improvement of Robustness of Adaptive Control," *Automatica*, Vol. 20, No. 5, 1984, pp. 583–594.

[46]Barkana, I. and Kaufman, H., "Direct Adaptive Control with Bounded Tracking Errors," *22nd IEEE Conference on Decision and Control*, Inst. of Electrical and Electronics Engineers, 1983.

[47]Barkana, I. and Kaufman, H., "Robust Simplified Adaptive Control for a Class of Multivariable Systems," *24th IEEE Conference on Decision and Control*, Inst. of Electrical and Electronics Engineers, 1985.

[48]Narendra, K. S. and Annaswamy, A. M., *Stable Adaptive Systems*, Springer-Verlag, Englewood Cliffs, NJ, 1989.

[49]Fomin, V. N., Fradkov, A. L., and Yakubovich, V. A., *Adaptive Control of Dynamical Systems*, Nauka, Moscow, 1981.

[50]Fehse, W., *Automated Rendezvous and Docking of Spacecraft*, Cambridge University Press, Cambridge, United Kingdom, 2003.

[51]Paluszek, M. and Thomas, S., "Generalized 3D Spacecraft Proximity Path Planning Using A*," *AIAA Infotech@Aerospace*, Arlington, VA, 2005, AIAA paper 2005-7043.

[52]Barkana, I. and Kaufman, H., "Global Stability and Performance of an Adaptive Control Algorithm," *International Journal of Control*, Vol. 46, No. 6, 1986, pp. 1491–1505.

[53]Fradkov, A. L., "Adaptive Stabilization of Minimal-Phase Vector-Input Objects Without Output Derivative Measurements," *Physiks-Doklady*, Vol. 39, No. 8, 1994, pp. 550–552.

[54]Fradkov, A. L., "Shunt Output Feedback Adaptive Controllers for Nonlinear Plants," *13th IFAC Triennial World Congress*, San Fransisco, CA, 1996, pp. 367–372.

[55]Iwai, Z. and Mizumoto, I., "Robust and Simple Adaptive Control Systems," *International Journal of Control*, Vol. 55, No. 6, 1992, pp. 1453–1470.

[56]Iwai, Z. and Mizumoto, I., "Realization of Simple Adaptive Control by Using Parallel Feedforward Compensator," *International Journal of Control*, Vol. 59, No. 6, 1994, pp. 1543–1565.

[57]Mizumoto, I. and Iwai, Z., "Adaptive Model Output Following Control for Plants with Unmodeled Dynamics," *33rd IEEE Conference on Decision and Control*, Inst. of Electrical and Electronics Engineers, 1994.

[58]Mizumoto, I. and Iwai, Z., "Simplified Adaptive Model Output Following Control for Plants with Unmodeled Dynamics," *International Journal of Control*, Vol. 64, No. 1, 1996, pp. 61–80.

[59]Nolet, S., "The SPHERES Navigation System: from Early Development to On-Orbit Testing," *AIAA Guidance, Navigation, and Control Conference and Exhibit*, Hilton Head, SC, 2007, AIAA paper 2007-6354.